

6. V. P. Bobkov et al., "Diffusion of heat during turbulent water flow with gas bubbles," *Inzh.-Fiz. Zh.*, 24, No. 5, 781-789 (1973).
7. M. Kh. Ibragimov, V. P. Bobkov, and N. A. Tychinskii, "Study of the behavior of a gas phase and gas in channels," *Teplofiz. Vys. Temp.*, No. 5, 1051-1061 (1973).
8. M. Kh. Ibragimov, G. I. Sabelev, and V. I. Sidorov, "Temperature field in a nonisothermal two-phase flow," *At. Energ.*, 28, No. 5, 421-422 (1970).
9. A. V. Zhukov, V. I. Subbotin, and P. A. Ushakov, "Heat transfer in the longitudinal flow of a liquid metal about parted bundles of rods," in: *Liquid Metals [in Russian]*, Atomizdat, Moscow (1967), pp. 149-169.
10. V. K. Koshkin et al., "Heat transfer in a channel containing a compact tube or rod bundle," *Teplofiz. Vys. Temp.*, 5, No. 2, 317-321 (1967).
11. P. P. Bobkov et al., "Heat transfer in the flow of water into a compact triangular rod bundle," *At. Energ.*, 37, No. 2, 127-130 (1974).

CERTAIN FEATURES OF TRANSVERSE FLOW ABOUT A CYLINDER
WITH LONGITUDINAL RIBS

L. N. Voitovich and A. G. Prozorov

UDC 532.526.5

It was experimentally established that the structure of the boundary-layer separation and the flow regime preceding separation can be influenced by installing longitudinal ribs on the surface over which flow is occurring.

It was shown earlier [1-4] that the free oscillation and vibration of structures in a liquid flow can be completely or partly damped by installing interceptors, transverse and oblique ribs, etc. on the surface about which flow is occurring. These devices change the character of separation of the boundary layer on the diffuser section of flow. The present work attempts to study the change in separated flow with the placement of lengthwise ribs on a wall, the ribs chosen so as to minimize the additional aerodynamic load on the structure.

The study was conducted in two wind tunnels with an open working part with nozzle diameters of 0.44 and 2.2 m. We used two circular cylindrical models with diameters $d_1 = 44$ mm and $d_2 = 160$ mm, respectively. Transverse flow over the models allowed us to clearly observe separation of the boundary layer from the initially hydraulically smooth surface. The smaller model No. 1 had a length $l = 634$ mm, and its ends were located beyond the limits of the flow in the working part of the tunnel. The length of the larger model No. 2 was 1080 mm, and its ends were fitted with a ring 0.36 m in diameter. The longitudinal ribs were rings of thickness $s_1 = 0.5$ mm and height $t = 0.5-9.0$ mm on model No. 1 and thickness $s_1 = 1$ mm and height $t = 4$ mm on model No. 2. The distance between the rings s_2 was varied within the range 3-75 mm.

The tests involved determination of the distribution of static pressure $p(\varphi)$ over the model surface and the total pressure $p_t(y)$ in its wake, as well as the intensity of the velocity pulsations $\varepsilon(\varphi)$ in the boundary layer a fixed distance $y \approx 0.5$ mm from the wall of the large model at different cross sections along its length. The total pressures in the wake behind the model were measured in cross sections where the flow was equalized along the length and the static pressure became almost equal to the pressure p_∞ in the unperturbed flow. The coefficients of profile drag of the cylinder c_x were calculated by the impulse method from the measured total pressures in the wake and the pressure distribution $p(y)$ on the surface of the model. In obtaining the measurements, we used a drainage system for the models, a rack of 23 pitot tubes, a constant-temperature hot-wire anemometer, and sliding traversing equipment.

The character of flow in the wake behind the cylinder was evaluated by installing a panel normal to the cylinder at different distances from it. The panel had silk threads

Translated from *Inzhenerno-Fizicheski Zhurnal*, Vol. 44, No. 3, pp. 368-372, March, 1983. Original article submitted June 1, 1981.

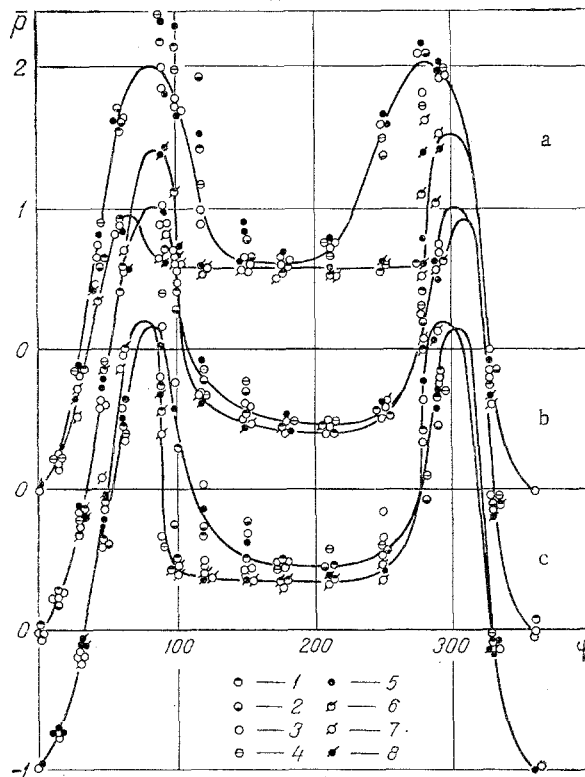


Fig. 1. Pressure distribution over the cylinder surface at different distances (mm) from the transverse symmetry plane of the model with ribs: 1) $z = -8$; 2) $z = -4$; 3) 0; 4) 4; 5) 8 and without ribs; 6) $z = -8$; 7) 0; 8) 8; a) $Re = 2.12 \cdot 10^5$; b) $3.63 \cdot 10^5$; c) 5.24×10^5 . φ , deg.

fastened to it at the nodes of a grid with cells measuring 10×10 mm. The diameter of the wire was 0.4 mm.

The experiments were conducted in the Reynolds number range $(0.67-5.70) \cdot 10^5$ corresponding to subcritical, critical and — at the maximum value $Re = 5.70 \cdot 10^5$ — supercritical regimes of flow about the cylinder.

The static pressure distribution $\bar{p}(\varphi)$ found on the model without ribs agrees well with data from other experiments (Fig. 1). The anemometric measurements (Fig. 2) show how an increase in the Reynolds number in the range $Re = (2.0-5.2) \cdot 10^5$ is accompanied in the flow just prior to separation by an increase in the intensity of the velocity pulsations in the boundary layer and development of the transition from laminar to turbulent flow. As a result, the separation is shifted downstream, beyond the "transition point," where the value of ϵ becomes maximal in the transitional region. In contrast to the case for high and low Re , at the critical Reynolds number $Re \approx 3.60 \cdot 10^5$ pressure is not constant on the aft part of the model surface; there are no $\bar{p} = \text{const}$ "ledges" on the curve $\bar{p}(\varphi)$ such ledges corresponding to the formation of a stagnant zone during separation of the boundary layer from the cylinder. The anemometric measurements nonetheless provide evidence of boundary-layer separation from the model wall at $\varphi = 110^\circ$ at this Reynolds number.

The installation of lengthwise ribs of a certain size on the models produces substantial changes in the pressure distributions and flow regime in the boundary layer on the cylinder surface. As an example, Figs. 1 and 2 show the distributions of pressure $\bar{p}(\varphi)$ and velocity pulsation intensity $\epsilon(\varphi)$ in the section $z = 0$ between two adjacent ribs halfway along model No. 2. Here $\bar{t} = 0.025$ and $\bar{s}_2 = 0.156$. Immediately evident on the curves $\bar{p}(\varphi)$ is the absence of the section $\bar{p} = \text{const}$ — a characteristic sign of the formation of an extensive stagnation zone near the wall. That which was an exception at $Re \approx 3.60 \cdot 10^5$ in the initial case is seen throughout the range of Reynolds numbers investigated on the cylinder with ribs. Together with the above, at $Re < 3.60 \cdot 10^5$ there is a marked increase in negative pressure in the model surface compared to the initial case, which usually occurs with a reduction in the

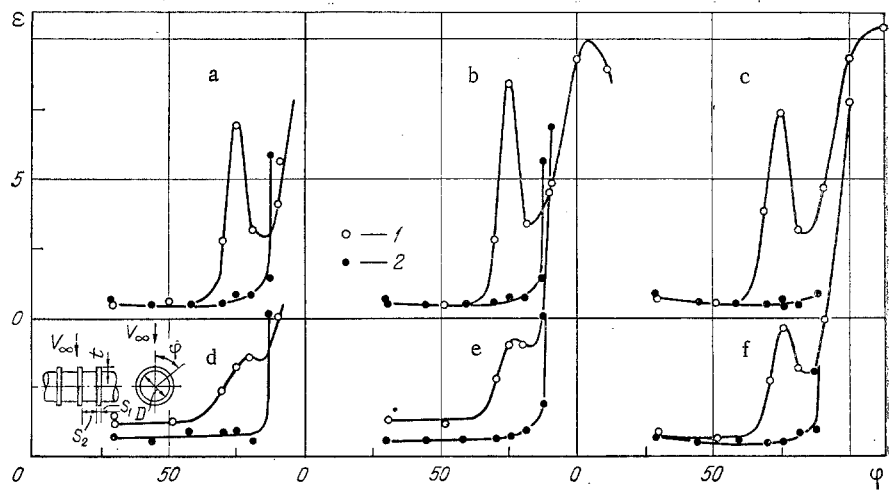


Fig. 2. Distribution of velocity pulsation intensity in the boundary layer on a cylinder without ribs (1) and with ribs (2): a) $Re = 4.19 \cdot 10^5$; b) $4.71 \cdot 10^5$; c) $5.21 \cdot 10^5$; d) $2.09 \cdot 10^5$; e) $3.07 \cdot 10^5$; f) $3.58 \cdot 10^5$. ϵ , %.

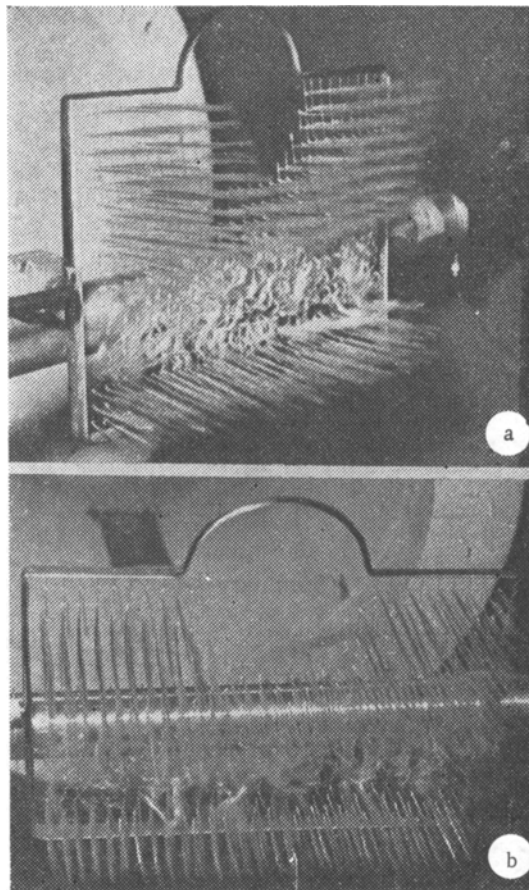


Fig. 3. Flow spectra in the near wake behind a cylinder without ribs (a) and with ribs (b).

width of the stagnant zone on a cylinder. The above-noted changes in pressure distribution are not connected, however, with a transition to the turbulent regime in the flow preceding separation, as was the case at $Re \approx 3.60 \cdot 10^5$ on the cylinder without ribs. Conversely, as can be seen from Fig. 2, the longitudinal ribs prevent the occurrence of a transition in the boundary layer up until its separation from the wall at the angle $\varphi = 81^\circ$. Thus, the pre-separation flow is stably relaminarized throughout the investigated Reynolds number range.

The above changes in flow, especially the increase in negative pressure, agree well with the determinations of the profile drag coefficients: c_x decreases compared to the initial case at Reynolds numbers $Re < 4 \cdot 10^5$ and increases at higher Re numbers. Thus, the coefficient is roughly 1.5 times lower than initially for model No. 1 with $Re = 1.28 \cdot 10^5$, $\bar{t} = 0.068$, and $\bar{s}_2 = 0.75$.

The measurements on model No. 1 showed that, approaching the longitudinal ribs, pressure on the cylinder surface becomes different from the pressure observed in the section $z = 0$. However, the character of the relation $\bar{p}(\varphi)$ remains the same as at $z = 0$, without "ledges." At the same time, the intensity of the velocity pulsations in the boundary layer is somewhat greater near the ribs than in the space between them. Judging from the above features of pressure distribution over the cylinder surface, it can be concluded that three-dimensional flow develops between the ribs.

Photographs of the flow spectrum in the near wake behind model No. 1 at $Re = 1.28 \cdot 10^5$ showed differences in turbulence behind the cylinder without ribs (Fig. 3a) and with ribs (Fig. 3b), where the pressure on the cylinder surface is similar to that shown in Fig. 1. The position of the threads on the panel show that the axes of the vortices, coincident with the model in the initial case, are direct parallel to the cylinder axis. Flow in the wake of the ribbed cylinder is clearly three-dimensional, with cells. A similar flow in the wake is evidently formed in the case of flow about a cylinder with a smooth surface without ribs with critical Reynolds numbers close to $Re \approx 3.60 \cdot 10^5$. In the case being examined, the wake flows obtained in determining pressure distributions and during visualization can be explained by their similarity to vortex models in which the axis is normal to the cylinder axis, as well as by a change in the structure of the stagnant zone near the model surface.

The effect of the ribs on transverse flow over the cylinder depends to a considerable degree on their relative height $\bar{t} = t/d$ and their spacing $\bar{s}_2 = s_2/d$ on the surface of the body. For example, on model No. 1 with $Re = 1.28 \cdot 10^5$ and changes in these parameters within the ranges $\bar{t} = 0-0.20$, $\bar{s}_2 = 0.068 - \infty$, the maximum reduction in profile drag was obtained at $\bar{t} = 0.068$, $\bar{s}_2 = 0.75$.

The above study results thus show that, through their appropriate installation on a surface over which flow with boundary-layer separation is occurring, longitudinal ribs can increase the buoyancy of the airfoil at low Reynolds numbers and critical or near-critical angles of attack, intensify mass transfer near the wall due to a change in the structure of the wake and stagnant zone, and relaminarize the flow preceding separation in the boundary layer.

NOTATION

d , diameter of cylinder model; l , length of cylinder model; t , height of longitudinal rib; s_1 , thickness of longitudinal rib; s_2 , distance between longitudinal ribs; φ , central angle of point of circumference reckoned from horizontal symmetry plane of model; x , coordinate reckoned along velocity vector of the unperturbed flow; y , coordinate reckoned along normal to horizontal symmetry plane of model or to its surface; z , coordinate reckoned along cylinder axis; p , static pressure; p_t , total pressure in flow; p_∞ and q_∞ , static and dynamic pressure in the unperturbed flow; $\bar{p} = (p - p_\infty)/q_\infty$, $\bar{p}_t = (p_t - p_\infty)/q_\infty$; ε , intensity of longitudinal component of velocity pulsations; c_x , coefficient of profile drag; v_∞ , velocity of unperturbed flow; ν , kinematic viscosity; $Re = v_\infty d/\nu$; $\bar{t} = t/d$; $\bar{s}_2 = s_2/d$.

LITERATURE CITED

1. V. K. Migai, "Studying ribbed diffusers," *Teploenergetika*, No. 10, 55-59 (1962).
2. K. K. Fedyavskii and L. Kh. Blyumina, *Hydrodynamics of Separated Flow About Bodies* [in Russian], Mashinostroenie, Moscow (1977).
3. I. N. Logvinov, S. A. Lukashchuk, and V. Ya. Fridland, "Improving the efficiency of aircraft control elements," in: *Certain Problems of Aerodynamics and Electrohydrodynamics* [in Russian], Vol. 7, KIIGA (Kiev Institute of Civil Aeronautical Engineering) (1971), pp. 103-106.
4. A. M. Mkhitarian, V. D. Trubenok, and V. Ya. Fridland, "Effect of the geometric parameters of swirlers on the drag of solids of revolution," in: *Certain Problems of Aerodynamics and Electrohydrodynamics* [in Russian], Vol. 3, KIIGA, Kiev (1968), pp. 81-87.